A Resonance Raman Study of the Copper Protein, Hemocyanin. New Evidence for the Structure of the Oxygen-Binding Site

Teresa B. Freedman,[1] Joann S. Loehr,[2] and Thomas M. Loehr*[1]

Contribution from the Department of Chemistry, Oregon Graduate Center, Beaverton, Oregon 97005, and the Department of Chemistry, Portland State University, Portland, Oregon 97207. *Received August 29, 1975*

Abstract: Resonance Raman spectroscopy of oxygen-carrying proteins, hemocyanins, by excitation within the ~570-nm band has permitted the identification of bound oxygen as O_2^{2-} and, hence, the oxidation states of copper as Cu(II). The frequency of the O_2^{2-} vibration is found at 744 cm^{-1} in *Cancer magister* (arthropod) and at 749 cm^{-1} in *Busycon canaliculatum* (mollusc) hemocyanins. Excitation profiles for the "peroxide" vibration consist of two components and indicate that the absorption and/or CD bands at ~490 and ~570 nm are due to $O_2^{2-} \rightarrow$ Cu(II) charge transfer. A molecular orbital scheme is presented in detail for a nonplanar Cu-O_2-Cu complex of C_2 symmetry which accounts for the diamagnetism and spectroscopy of oxyhemocyanin. Laser excitation into the ~340-nm band gives rise to resonance Raman peaks at 282 and 267 cm^{-1}, respectively, for the oxyhemocyanins from the two phyla. These frequencies are assigned to Cu-N(imidazole) vibrations of histidine ligands. Resonance enhancement profiles for these low frequency modes indicate that the ~340-nm band of oxyhemocyanin may be assigned to charge transfer between N(imidazole) and Cu(II). Our analysis of presently available spectroscopic data of arthropod and molluscan hemocyanins suggests that differences in these proteins may simply be due to slight geometric alterations rather than structural differences in the O_2 binding sites.

The properties of hemocyanin, the oxygen-carrying protein in the hemolymph of many molluscs and arthropods, have been extensively investigated, including amino acid composition, subunit structure, oxygen binding equilibria, and spectral characteristics.[3-5] Although it is known that one oxygen molecule binds to two copper ions in the protein, the structure of the copper-oxygen complex has not been established. Various assignments of the absorption bands of blue oxyhemocyanin at ~345 nm ($\epsilon_{Cu} \simeq 10\,000$) and ~570 nm ($\epsilon_{Cu} \simeq 500$) exist in the literature.[6,7] While antiferromagnetic coupling of Cu(II) ions has been postulated to explain the diamagnetism of the oxygenated protein,[7,8] the mechanism of the copper-copper interaction has not been determined.

Direct information on the nature of metal-ligand interactions can be obtained from the assignment of vibrational modes observed by infrared or Raman spectroscopy. For metalloproteins with strong absorption bands in the visible and near-uv, resonance Raman spectroscopy has made possible not only the elucidation of the structure of the metal binding sites but also the assignment of the electronic transitions associated with these absorption bands.[9]

In a preliminary report,[10] we presented a partial assignment of the resonance Raman spectrum of *Cancer magister* hemocyanin. Since observed differences between molluscan and arthropod hemocyanins seem to suggest dissimilar oxygen binding site structures,[4,11-13] we have extended our study to compare the resonance Raman spectrum of hemocyanin from the mollusc, *Busycon canaliculatum*, to that of the arthropod, *Cancer magister*. We present here assignments of the Raman and uv-visible spectra. In addition, we propose a structure for the oxygen binding site and a molecular orbital scheme which accounts for many of the spectral and magnetic properties of hemocyanin.

Experimental Section

Hemocyanin was prepared from the Pacific crab, *Cancer magister* (Edmund's, Garibaldi, Ore.), and the channeled whelk, *Busycon canaliculatum* (Marine Biological Laboratory, Woods Hole, Mass.).

Hemolymph from *C. magister* was centrifuged at 12 000*g* for 10 min to remove clotted protein. The hemocyanin in the supernatant was sedimented by centrifuging 4 h at 165 000*g* and the pellet was dissolved overnight in a few milliliters of buffer (0.01 M Tris-Cl, 0.01 M $MgCl_2$, 0.05 M $NaClO_4$, pH 8.5; or 0.05 M carbonate, 0.05 M $NaClO_4$, pH 9.8). The resulting solution was centrifuged 20 min at 32 000*g* to remove undissolved protein, sterilized by passage through a 0.45 μm Millipore filter and stored in sterile bottles. Hemocyanin concentrations were 50-100 mg/ml (1.3-2.5 mM Cu). Storage of the protein for several weeks at 4 °C had little effect on the quality of Raman spectra other than an increase in background and slight diminution of signal.

The *B. canaliculatum* hemolymph was centrifuged at 12 000*g* for 10 min. The supernatant was dialyzed against buffer (listed above) and concentrated to ca. 75 mg/ml (3 mM Cu) by ultrafiltration through a Millipore Pellicon filter. The dialyzed *B. canaliculatum* hemocyanin was quite turbid and caused excessive light scattering at pH 8.5, but became transparent at pH 9.8 upon subunit dissociation. Clear samples were also obtained by centrifuging the hemolymph supernatant 1-2 h at 165 000*g* and carefully redissolving the pellet by slow addition of distilled water to form a concentrated sample of ca. 160 mg/ml (6.3 mM Cu). *Busycon* samples were used within a week of their preparation since background scattering increased markedly with longer storage at 4 °C.

Hemocyanin concentrations were determined spectrophotometrically (Cary Model 16) using ϵ_{345} 10 000 M^{-1} (Cu) cm^{-1} for *Busycon*[12] and ϵ_{340} 10 000 M^{-1} (Cu) cm^{-1} for *Cancer* hemocyanin.[8]

Deoxygenation was carried out on a 0.2-ml sample in a 5-ml chamber by alternating slow evacuation and equilibration with N_2 (Airco prepurified) saturated with water vapor. The $^{18}O_2$ hemocyanin was prepared by equilibrating the colorless deoxyhemocyanin with $^{18}O_2$ (Miles Laboratories, 91.07 atom % ^{18}O) at ~200 Torr.

Apohemocyanin (*Cancer*) was prepared by the method of Thomson et al.[14] Methemocyanin and NO-hemocyanin (60-150 mg/ml) from *C. magister* and *Helix pomatia* were kindly provided by Dr. H. van der Deen. We were unable to obtain resonance Raman spectra of NO-hemocyanin or methemocyanin due to their fluorescence and to the absence of intense charge transfer bands in the visible region in these samples.

Literature methods were used to prepare the μ-peroxocopper(II) compound $[Cu(OH)]_2(OOH)(CH_3COO)$,[15] $Cu(Im)_4Cl_2$[16] (where Im = imidazole), $Cu(Im)_4(NO_3)_2$,[16] and $Cu(1,2\text{-}Me_2Im)_2Cl_2$.[17] Copper poly-L-histidine[18] (~30 mg/ml) was made in 0.05 M acetate buffer (pH 5.0) from $CuCl_2 \cdot 2H_2O$ and poly-L-histidine (Sigma, degree of polymerization ~110) at a 1:5 copper to histidine mole ratio.

Raman spectra were recorded on a Jarrell-Ash 25-300 Raman spectrophotometer equipped with a Coherent Radiation (CR) Model 52MG Ar^+/Kr^+ laser (457.9, 488.0, 496.5, 514.5, 520.8, 530.9, 568.2, and 647.1 nm) or a CR Model 52 Ar^+ laser (457.9, 476.5, 488.0, and 514.5 nm). Plasma lines were eliminated with spike filters. Laser power at the sample was maintained below 120 mW to minimize sample deterioration.

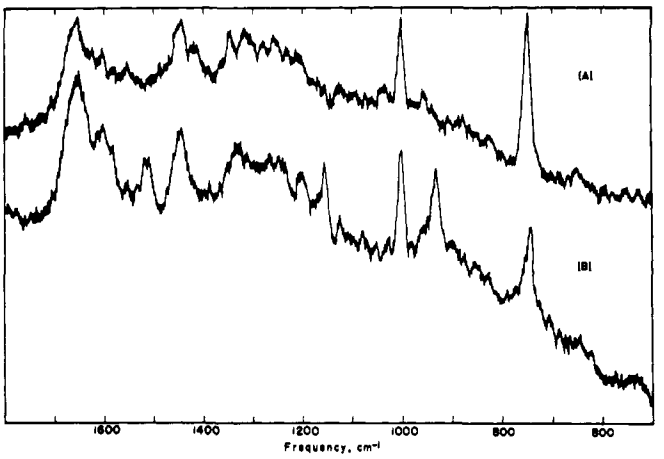

Figure 1. Raman spectra of oxyhemocyanin using 530.9-nm excitation, 20 cm^{-1}/min scanning rate, 5-s time constant, 8-cm^{-1} spectral slit width: (A) *Busycon canaliculatum* oxyhemocyanin, 165 mg/ml, pH 9.8; (B) *Cancer magister* oxyhemocyanin, 60 mg/ml, pH 8.5. Peak at 932 cm^{-1} is ν_1 (ClO_4^-). Peaks at 1160 and 1520 cm^{-1} are due to impurity (see text).

Raman spectra of the protein solutions and poly-L-histidine complex were obtained at room temperature in 1.7-mm capillary tubes or in the side arm (10 × 5 mm o.d.) of the deoxygenation chamber. A 90° scattering geometry was employed. Intensities were measured as peak heights relative to ν_1(ClO_4^-) (internal standard) at 932 cm^{-1} or relative to the 1003-cm^{-1} protein (phenylalanine) vibration.

Raman spectra of the Cu complexes, mounted in a spinning sample holder as pure solids or mixed with KNO_3 for an internal standard, were recorded using a ~180° scattering geometry.

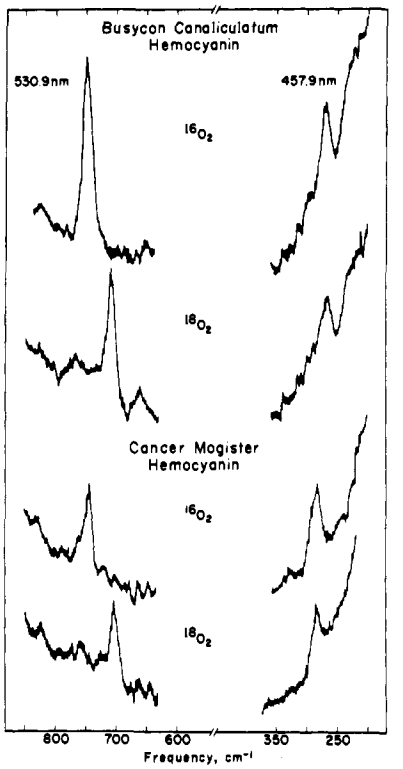

Figure 2. Raman spectra of $^{16}O_2$- or $^{18}O_2$-hemocyanin, using 530.9- or 457.9-nm excitation; conditions are as in Figure 1.

Raman Spectral Studies and Assignments

Effect of pH on Raman Scattering. *Busycon* hemocyanin at pH 8.5 (75 mg/ml) produced such a high background signal due to light scattering from its large molecules (100S)[19] that the Raman spectrum was obscured. Dissociation of the protein at pH 9.8 into 60S and 15S subunits[19] resulted in an optically clear solution satisfactory for Raman spectroscopy. Excellent spectra were also obtained using clear gels of *Busycon* hemocyanin (160 mg/ml, pH 8). *Cancer* hemocyanin solutions were clear at either pH. Variation in pH from 8.5 to 9.8 caused no apparent shifts in the positions of the Raman peaks in either *Cancer* or *Busycon* hemocyanin. The Raman spectra of oxyhemocyanin from *B. canaliculatum* and *C. magister* are compared in Figure 1 for the 500–1800-cm^{-1} range, and in Figure 2 for the 200–350-cm^{-1} range.

Nonresonant Raman Spectral Peaks. The majority of the peaks observed in the Raman spectra of *Cancer* and *Busycon* oxyhemocyanin are also present in the deoxygenated and copper-free forms of *Cancer* hemocyanin. The intensities of these peaks, measured relative to the ν_1 mode of ClO_4^- at 932 cm^{-1}, are independent of excitation wavelengths between 457.9 and 647.1 nm. By comparison with Raman spectra of other proteins, the nonresonant peaks can be assigned to vibrations of specific amino acid side chains and the protein backbone.[20] For example, the strong, sharp peak at 1003 cm^{-1} is a ring vibration due to phenylalanine, and the more complex peaks at ~1660 and ~1250 cm^{-1} are assigned to the amide I and amide III vibrations, respectively. Weaker features are generally attributed to tryptophan, tyrosine, and other phenylalanine vibrations. The amino acid content of arthropod and molluscan hemocyanins (normalized to molecular weight) is essentially identical,[21] especially for the aromatic residues which dominate the Raman spectra. The dissimilarities in the intensities of nonresonant peaks could be indicative of minor conformational differences among the proteins of the two phyla. The appearance of a protein spectrum in addition to resonance-enhanced Raman peaks is unusual for metalloproteins and is due to the high protein concentrations needed to compensate for the low absorption of hemocyanin solutions in the visible region.

Resonance Raman Peaks. The *C. magister* hemocyanin Raman peaks at 744 and 282 cm^{-1} are observed *only* in the oxy form; they are absent in the spectra of both the deoxy- and apoproteins. The intensities of these peaks, and of the corresponding peaks at 749 and 267 cm^{-1} in *B. canaliculatum* oxyhemocyanin, exhibit a pronounced dependence upon excitation wavelengths, as plotted in Figure 3. A comparison of the sensitivity of these peaks to O_2 isotope substitution is shown in Figure 2.

A. The 700-cm^{-1} Region. The intensity-enhancement profiles (Figure 3B and 3D) for the Raman peaks in the 700-cm^{-1} region suggest that resonance is not with a single electronic band but with two overlapping transitions. The shoulder and maximum in the profile for the *Busycon* hemocyanin 749-cm^{-1} peak correspond closely to the circular dichroism (CD) spectral bands observed at 486 (+) and 558 nm (−) (Table I). In *Cancer magister* hemocyanin the shoulder in the 744-cm^{-1} excitation profile matches well with the positive CD band at 507 nm, while the maximum in the profile appears to correspond to the 575-nm visible absorption band (Table I). CD spectra of arthropod hemocyanins lack a distinct band at 575 nm.[11] However, the appearance of this electronic transition in both *Cancer* and *Busycon* Raman excitation profiles makes it likely that a transition near 570 nm in the CD spectra of arthropod hemocyanins is not resolved from the positive bands at ca. 490 and 615 nm.

The Raman peaks at 744 cm^{-1} in *Cancer* and 749 cm^{-1} in *Busycon* oxyhemocyanins are sensitive to oxygen isotope, shifting to 704 and 708 cm^{-1}, respectively, in the $^{18}O_2$-enriched samples (Table II). The ratio of the frequencies of these resonance Raman peaks in $^{16}O_2$- and $^{18}O_2$-hemocyanin equals 1.058 in *Busycon* and 1.057 in *Cancer* hemocyanin. Since the theoretical ratio of the vibrational stretching frequencies of the isotopes of diatomic oxygen is $\nu(^{16}O_2)/\nu(^{18}O_2)$ = 1.061,

Table I. Spectral Properties of Oxyhemocyanins and Their Assignments

Protein source	Method[a]	Temp (°K)	Absorption bands (nm): Ligand → Cu(II) charge transfer		O_2^{2-} → Cu(II) charge transfer		d–d transitions	
C. magister	Abs[b]	298	340	—	—	575	—	—
	Abs[c]	5	*h*	425	—	560	605	675
	CD[d]	298	338	~440[i]	507	—	608	—
	RR[e]	298	~340		505	570		
B. canali-culatum	Abs[f]	298	345	—	—	570	—	—
	CD[g]	298	345	~430[i]	486	558	—	708
	RR[e]	298	~345		485	550		

[a] Key: Abs = absorption spectrum; CD = circular dichroism spectrum; RR = resonance Raman intensity enhancement profile (from Figure 3). [b] Reference 8. [c] Reference 22. [d] H. D. Ellerton and K. E. van Holde, unpublished results, 1970. [e] This work. [f] Reference 12. [g] Reference 11. [h] Not measured. [i] Weak shoulder on the ~495-nm CD band.

Table II. Resonance Raman Peaks (cm^{-1}) of Hemocyanins

Source	$^{16}O_2$-hemocyanin	$^{18}O_2$-hemocyanin
C. magister	744	704
	282	282
B. canali-culatum	749	708
	267	267

we assign these resonance enhanced Raman peaks in hemocyanin to the stretching vibration of the bound oxygen.

Vibrational frequencies in the region 700–850 cm^{-1} have been assigned to peroxide stretch in anhydrous Na_2O_2, 738 cm^{-1},[23] and in μ-peroxo binuclear Co(*III*) complexes, ~800 cm^{-1}.[24] We have observed a single, weak peak at 810 cm^{-1} in the Raman spectrum of a cupric peroxide complex presumed to be a polymer of the form

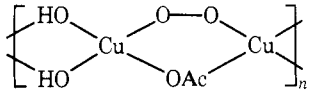

This brown precipitate, the reaction product of cupric acetate and H_2O_2, is diamagnetic and has weak electronic bands near 370 and 700 nm.[15] No intensity enhancement was observed for its 810-cm^{-1} Raman peak (measured relative to the 720-cm^{-1} peak of the KNO_3 internal standard) with laser excitation in the range 457.9–647.1 nm.

Our Raman spectroscopic results are strong evidence that oxygen is bound as a peroxide ion, O_2^{2-}, in oxyhemocyanin. Since numerous studies have indicated that deoxyhemocyanin contains Cu(I) ions,[4] oxygen binding as an oxidative addition to form peroxide ion suggests the presence of Cu(II) in oxyhemocyanin. The low vibrational frequency for the peroxide ion in hemocyanin is in accord with observations that the coppers are bound in a strongly hydrophobic environment.[25] A similar analysis of bound oxygen as peroxide has been made for oxyhemerythrin in which a resonance Raman peak is observed at 844 ($^{16}O_2$) and 798 cm^{-1} ($^{18}O_2$).[26]

In Raman scattering, for a vibration to undergo resonance enhancement by an electronic transition, the geometry of the molecule must change along the normal coordinate of that vibration in transition from the ground to the excited electronic state.[27] It is, therefore, likely that visible and/or CD transitions in *Busycon* and *Cancer* hemocyanins near 490 and 570 nm involve O_2^{2-} → Cu(II) charge transfer, which strengthens the O–O bond and leads to enhancement of this vibrational mode.

B. The 200-cm^{-1} Region. The frequency of the second resonance-enhanced Raman peak in oxyhemocyanin, at 282 cm^{-1} in *Cancer* and at 267 cm^{-1} in *Busycon*, is insensitive to $^{18}O_2$ substitution (Table II; Figure 3). No such peak is observed in deoxy- or apohemocyanin of *C. magister*. The relative intensities of these peaks agree well with the theoretical resonance behavior[10,28] of a ~280-cm^{-1} vibration in resonance with a 340 nm (*Cancer*) or 345 nm (*Busycon*) electronic transition, as shown in Figures 3A and 3C. With 568.2- and 647.1-nm excitations, however, the relative intensity of the 282-cm^{-1} peak in *Cancer* hemocyanin deviates from the theoretical line, suggesting a slight resonance enhancement from the ~610-nm transition.

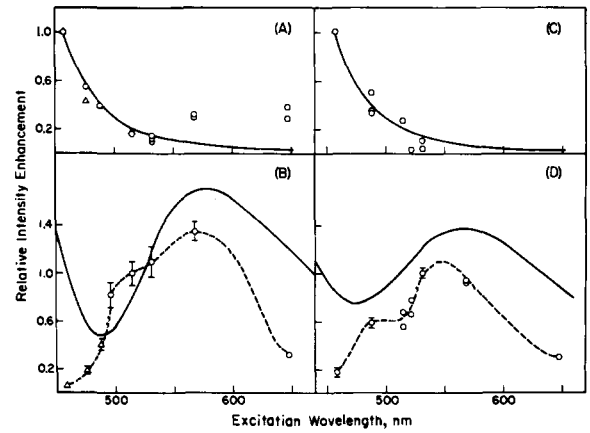

Figure 3. Relative intensity enhancement profiles. (A) *C. magister* hemocyanin, 282-cm^{-1} peak, normalized to relative intensity with 457.9-nm excitation. Solid line is the theoretical curve for ν_e = 340 nm, $\Delta\nu$ = 282 cm^{-1} (ref 28). (B) *C. magister* hemocyanin, 744- and 704-cm^{-1} peaks, normalized to relative intensity with 514.5-nm excitation. Solid line is the absorption spectrum, arbitrary ordinate scale. (C) *B. canaliculatum* hemocyanin, 267-cm^{-1} peak, normalized to relative intensity with 457.9-nm excitation. Solid line is the theoretical curve for ν_e = 345 nm, $\Delta\nu$ = 267 cm^{-1} (ref 28). (D) *B. canaliculatum* hemocyanin, 749-cm^{-1} peak, normalized to relative intensity with 530.9-nm excitation. Solid line is the absorption spectrum, arbitrary ordinate scale. Symbols: △, $^{18}O_2$-hemocyanin; ○, $^{16}O_2$-hemocyanin. Error bars indicate average deviations for three or more experiments.

Our oxygen isotope substitution experiments show that these Raman peaks are due to vibrations which are associated with the copper ions and their ligands, but which do not involve the bound peroxide ion. Frequencies in the 250–290-cm^{-1} region have been assigned to copper–nitrogen stretching vibrations in Cu–imidazole complexes (Table III). Moreover, these complexes exhibit strong ultraviolet bands between 310 and 360 nm. Bryce and Gurd[31] have suggested that Cotton effects in the near-uv (300–350 nm) for Cu(II) complexes of histidine-containing peptides are associated with charge transfer between copper and imidazole. The pH 5 complex of Cu(II) with poly-L-histidine (PLH) reported by Levitzki et al.,[18] containing three imidazole ligands, also has an absorption between 350 and 380 nm. We have prepared the Cu(II)–PLH complex at pH 5 and find a uv shoulder between 300 and 350 nm; the Raman spectrum of this deep blue solution shows a

Table III. Spectral Properties of Some Copper-Imidazole Complexes and Copper-Proteins

Compound[a]	Stereochemistry	ν_{Cu-N} (cm^{-1}) Infrared	ν_{Cu-N} (cm^{-1}) Raman[b]	Uv absorption (nm)
$Cu(Im)_4Cl_2$	Dist. octahedral	286[c]	245	309[d]
$Cu(Im)_4(NO_3)_2$	Dist. octahedral	292[c]	250	310[d]
$Cu(MeIm)_2Cl_2$	Tetrahedral	271[c]		362[c]
$Cu(MeIm)_2Br_2$	Tetrahedral	274[c]		355[c]
$Cu(MeIm')_2$		275[c]		350[c]
$Cu(MeIm)_4Cl_2$	Dist. octahedral	275[c]		
$Cu(Me_2Im)_2Cl_2$	Tetrahedral	261, 242[e]	255	349[e]
$Cu(BrIm)_2Cl_2$	Dist. octahedral	275[f]		
$Cu(BrIm)_2Br_2$	Dist. octahedral	275[f]		
Cu(poly-L-histidine)	Dist. octahedral		~260	350–380[g]
Oxyhemocyanin:				
C. magister			282	340
B. canaliculatum			267	345

[a] Key: Im = imidazole; MeIm = 2-methylimidazole; Im' = imidazolate anion; Me_2Im = 1,2-dimethylimidazole; BrIm = 4(5)-bromoimidazole. [b] This work. [c] Reference 29. [d] Reference 16. [e] Reference 17. [f] Reference 30. [g] Reference 18.

weak peak near 260 cm^{-1} when using 488.0- and 457.9-nm laser excitations.

Since the spectral properties of these systems correlate well with the uv and Raman spectra of hemocyanin, we assign the low frequency resonance Raman peak at 282 or 267 cm^{-1} in oxyhemocyanin to the Cu-N(imidazole) vibration of coordinated histidines. Furthermore, we conclude that the ~340-nm transition of oxyhemocyanin (which is responsible for resonance enhancement of these Raman modes), must involve charge transfer between N(imidazole) and Cu(II). Based on the excellent fit of the observed relative intensities to enhancement by a *single* electronic transition (Figures 3A and 3C), only the totally symmetric Cu-N vibrations should be enhanced.[28] Therefore, we cannot determine the number of histidine ligands from our Raman studies. The 282- and 267-cm^{-1} Raman peaks are, however, asymmetric indicating two or more histidines bound at slightly inequivalent sites.

The present Raman spectroscopic results are in accord with previous suggestions for the existence of histidine ligands to copper ions both in model compounds and in hemocyanin. Structural investigations by Freeman and co-workers[32] with Cu(II) and histidine containing peptides have shown the propensity of Cu(II) to bind to the imidazole group. In their opinion, three characteristics of imidazole which make it an attractive ligand are: (1) the flexibility of the metal-nitrogen bond; (2) the electron donor strength of the ring nitrogen, and (3) the ionization state of imidazole at physiological pH's. Evidence that each copper ion in hemocyanin is bound to four histidine groups has been obtained from acid-base titrations of molluscan and arthropod hemocyanins.[25] The presence of at least two nitrogen ligands per copper has been inferred from the superhyperfine structure of the EPR spectrum of NO-hemocyanin.[33] Other chemical and physical modifications of the protein have also implicated histidine involvement at the oxygen-binding site.[34,35]

Alternative assignments for the 267- or 282-cm^{-1} Raman peaks are much less attractive. While this frequency region is satisfactory for a Cu-S[36] or Cu-O(carboxylate)[37] vibration, there exists little or no evidence for the presence of cysteine sulfhydryl groups[14,21] or carboxylate side chains[25] at the metal-binding site in hemocyanin. Furthermore, methionine-SCH_3 groups do not coordinate Cu(II) in model Cu(II)-methionine complexes.[32] Whereas Cu-N(peptide) and Cu-O(peptide) bonds have been observed in structural investigations of Cu(II) complexes,[32] the stretching frequencies of such bonds have been placed[38] in a range of 350–400 cm^{-1}, markedly higher than are observed here. Cu-N(amino) frequencies are assigned at even higher values.[36] Tyrosine and tryptophan residues may be located near the hemocyanin copper ions[35,39,40] stabilizing the hydrophobic oxygen binding site,[25] but the high pK's of the phenol oxygen and the indole nitrogen make them unlikely copper ligands.

C. Further Spectral Assignments. With 647.1-nm laser excitation, the total hemocyanin Raman spectrum is extensively attenuated, a phenomenon we have observed when irradiating within d-d bands of other copper complexes. This observation, together with the moderate resonance enhancement with the 647.1-nm line of the 282-cm^{-1} peak (Figure 3A), suggests that the visible and CD bands of hemocyanin in the 600–700-nm region (Table I) are d-d transitions which have gained intensity due to mixing with the low-lying ~340-nm charge transfer transition.

The 425-nm absorption peak resolved in the 5 K spectrum of *C. magister* hemocyanin[22] (Table I) is similar in energy to the shoulders at 410 and 440 nm in the 77 K spectrum of ceruloplasmin.[41] These weak absorptions may arise from a ligand → Cu(II) charge transfer transition in addition to the one observed at ~340 nm for hemocyanin. However, contributions from a peak at 425 nm to the intensity enhancement profile for the ~282-cm^{-1} peak of hemocyanin would be negligible in comparison to the contribution from the ~340-nm transition. The resonance Raman excitation profiles do show that the 426-nm band is *not* involved in the enhancement of the ~740-cm^{-1} peak and, thus, this absorption band is *not* assignable to O_2^{2-} → Cu(II) charge transfer.

A strong absorption band near 330 nm is observed in the multicopper enzymes laccase, ceruloplasmin, ascorbate oxidase,[42] and oxytyrosinase.[43] By analogy to our hemocyanin spectral interpretations, this band may also result from the coordination of histidine ligands to the antiferromagnetically coupled coppers in these enzymes.

D. A Possible Polyene Contaminant. In several hemocyanin preparations from *C. magister*, Raman peaks appeared at 1520 and 1160 cm^{-1} which varied in their intensities between different preparations and were not proportional to nonresonant protein peaks, e.g., the 1003-cm^{-1} phenylalanine peak. They exhibited resonance enhancement, maximizing in intensity with 530.9-nm excitation; they were observed with all blue and green excitations but were no longer seen with 568.2 nm and longer wavelengths. We ascribe these peaks to a small amount of contaminative substance which is possibly carotenoid in nature, since lycopene[44] and photoreceptor pigments[45] exhibit resonance enhanced peaks close to these frequencies at concentrations as low as 10^{-7} M. We were unable to extract the contaminant into hexane from freeze-dried *C. magister* hemocyanin, suggesting that the substance either is covalently bound to the hemocyanin or is part of a protein which centrifuged with the hemocyanin. Peaks near the same frequencies, assigned to unidentified contaminants, have been observed in the Raman spectra of membrane fractions (ghosts) from both human red cells[46] and invertebrate erythrocytes (*Golfingia gouldii*).[47]

Discussion

Comparison of Mulluscan and Arthropod Hemocyanin. While arthropod and molluscan hemocyanins both function as oxygen carriers, differences in a number of their properties

(see below) have led to the conclusion that the O_2-binding sites in arthropod and molluscan hemocyanins must differ significantly. However, our resonance Raman study shows that the mode of oxygen binding, oxidative addition of oxygen, is the same for the two phyla, and the small difference in the vibrational frequencies of the bound O_2^{2-}, 749 cm^{-1} in *Busycon* vs. 744 cm^{-1} in *Cancer* hemocyanin, suggests that the oxygens are bound in rather similar environments. While the difference in frequency of the copper-ligand vibration, 282 vs. 267 cm^{-1}, is somewhat larger, the ligands (histidine) are undoubtedly the same for hemocyanins in the two phyla.

Many of the phylogenetic differences which have been observed among hemocyanins could be explained by assuming slightly different protein conformations and copper site geometries rather than different chemical structures of the oxygen binding sites. Thus, opposite signs in the 260–295-nm region of CD spectra[11] as well as dissimilar quaternary structures seen in electron micrographs[3,4] and different molecular weights[48] may simply reflect variances in protein conformations. Dissimilarities at the copper sites themselves are observed in variation of Cu–Cu distances as estimated from EPR spectra of NO-hemocyanin (5.7 ± 0.2 Å for *C. magister* and 6.4 ± 0. 3 Å for *H. pomatia*),[33] in differences in CD bands of oxyhemocyanins (bands at approximately 485 (+), 565 (−), and 710 nm (+) for molluscs and at 490 (+) and 615 nm (+) for arthropods),[11] and in the strengths of CO binding.[13,49] The great diversity in hemocyanin affinities for O_2 appears to correlate more with organism life style than evolutionary relationship,[3,4] indicating that species differences in oxygen affinity may involve small changes in copper site geometries without necessitating changes in copper ligands.

Models for the Oxygen Binding Site. Several geometries for the binding of an oxygen molecule to two copper ions can be proposed (Chart I). Molecular orbital (MO) schemes have been previously proposed for some of the bridging geometries[5,7,8] to illustrate the nature of the antiferromagnetic coupling in hemocyanin and to suggest various assignments of the 340- and 570-nm transitions. In view of the new evidence from our Raman investigations for the oxidation states of copper and oxygen and the assignment of electronic bands in oxyhemocyanin, we have considered how the highest energy d orbitals of the coppers interact with the oxygen molecular orbitals for the various geometries, and what predictions can be made from the resultant estimated molecular orbital energy diagrams.

Chart I

I. μ-Dioxygen Bridging

(a) planar, C_{2v} (cis)

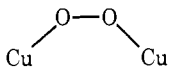

(b) planar, C_{2h} (trans)

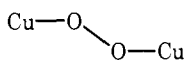

(c) nonplanar, C_2

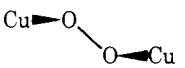

(d) π-bridged;
planar, D_{2h}, or nonplanar, C_{2v}

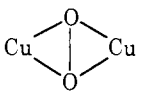

II. μ-Monooxygen Bridging

(a) planar, C_{2v}

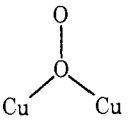

(b) nonplanar, C_s

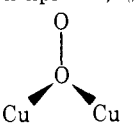

III. Terminal Oxygen Binding

(a) monodentate, nonlinear

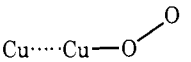

(b) bidentate, π-bonded

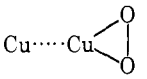

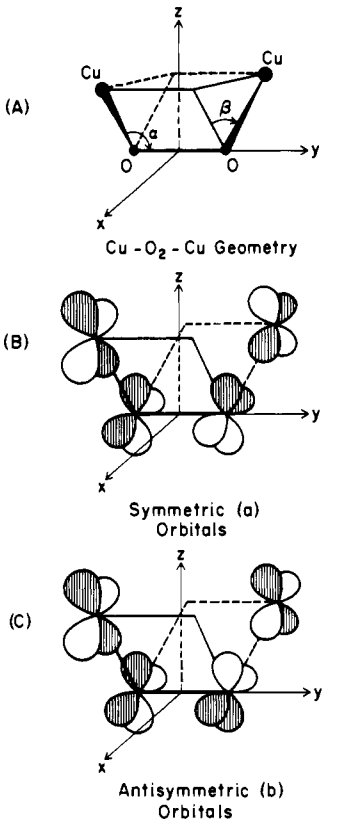

Figure 4. (A) Geometry (Ic) for nonplanar, μ-dioxygen bridged Cu–O_2–Cu complex; C_2 symmetry, twofold axis along z; α and β are the Cu–O–O and dihedral angles, respectively. (B) Symmetric (a) combination of copper d_{xy} orbitals and oxygen p_x and p_z orbitals; $\beta \simeq 90°$. (C) Antisymmetric (b) orbitals.

We have patterned our analysis on a recent theoretical study of magnetic coupling in copper dimers. For μ-bridged Cu(II) ions, Hay, Thibeault, and Hoffmann[50] calculate the energy splitting between the symmetric and antisymmetric combinations of the half-filled d orbitals, ϕ_S and ϕ_A, respectively, due to antibonding interaction with the highest energy orbitals of the proper symmetries on the briding atom or group. The magnitude of the splitting, $|\Delta E| = |E(\phi_S) - E(\phi_A)|$, correlates with the energy difference between the singlet and triplet states of the copper dimer. For $|\Delta E| \simeq 0$, the triplet state is lower in energy; for large $|\Delta E|$, the dimer has a singlet ground state and exhibits antiferromagnetic behavior.

For oxyhemocyanin, μ-dioxygen bridged structures (I) have often been proposed. Since the nonplanar, C_2 configuration (Ic) appears to be the most stable for a peroxo bridge, e.g., hydrogen peroxide[51] and μ-peroxo binuclear Co(III) complexes,[52] we have adopted this geometry as a structural model and will present our MO analysis in detail.

In Figure 4 we consider the σ-bonding interaction of the highest energy copper d orbitals (primarily d_{xz} for the coordinate axes shown) with the oxygen orbitals, where the dihedral angle, β, is near 90°. For C_2 symmetry, Figure 4B shows the symmetric orbitals of species a (symmetric to twofold rotation about the z axis) and Figure 4C the antisymmetric orbitals of species b. The degenerate bonding π_u and antibonding π_g orbitals in the free oxygen molecule are each split into an a and b component under C_2 symmetry. As seen from Figure 4 and the MO scheme in Figure 5, each of these oxygen orbitals should be stabilized by bonding interaction with the copper d orbitals. The σ_g (bonding) oxygen orbitals, also of a species in C_2 symmetry, interacts with the other a orbitals and is probably raised in energy (cf. H_2O_2[53] and O_2[54]). The a and b antibonding combinations ϕ_S and ϕ_A, of the copper d orbitals with oxygen orbitals which are localized primarily on the coppers,

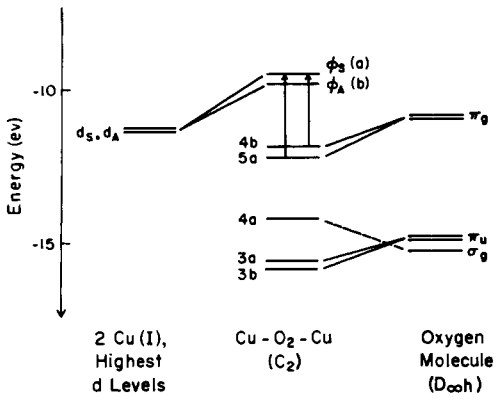

Figure 5. Molecular orbital scheme for Cu-O_2-Cu, C_2 symmetry. Interaction of symmetric (d_S) and antisymmetric (d_A) combinations of the highest energy copper d levels with oxygen $3\sigma_g$, π_u, and π_g molecular orbitals. Energies estimated from ref 50, 53, and 55. Oxygen MO's $1\sigma_g$, $1\sigma_u$, $2\sigma_g$, and $2\sigma_u$, and Cu-O_2-Cu orbitals 1a, 1b, 2a, and 2b lie at much lower energies and are not included in the diagram. Other Cu d levels are excluded for clarity. Transitions indicated are allowed $O_2^{2-} \rightarrow 2Cu(II)$ charge transfer assigned at ~490 and ~570 nm in hemocyanin.

are increased in energy from that in the isolated copper ions. The extent of splitting in energy of the a and b pairs derived from the oxygen π_u and π_g and copper d orbitals will be determined by the deviation of the dihedral angle from 90° and the strength of the Cu-O bond. The energies of the molecular orbitals for Cu-O_2-Cu given in Figure 5 are reasonable estimates based on calculations for H_2O_2,[53] copper dimers,[50] and Cu(II) complexes.[55]

If we now consider the bridging of two Cu(I) ions (four electrons in the highest d levels on the two Cu's) by molecular oxygen (eight electrons in the interacting orbitals), we must accommodate 12 electrons in the molecular orbitals of Cu-O_2-Cu shown in Figure 5. Our MO scheme illustrates that (a) the oxygen is bound as peroxide, since all the levels primarily localized on oxygen are filled, (b) the copper will be present as Cu(II) since the two copper d levels share only two electrons, and (c) the complex is diamagnetic, assuming that the separation between levels ϕ_A and ϕ_S is large enough to have ϕ_A doubly occupied and ϕ_S empty at room temperature. Magnetic susceptibility measurements[56] on oxyhemocyanin place the lower limit of the exchange coupling at 625 cm^{-1}.

In addition to accounting for the magnetic properties, oxidation states, and O_2 vibrational frequency in hemocyanin, the MO diagram for the C_2 configuration can be used to interpret the absorption and CD spectra and the resonance behavior of the peroxide vibration. The z-polarized charge transfer transition, $O_2^{2-} \rightarrow$ Cu(II) [**5a** $\rightarrow \phi_S$], and the x,y-polarized transition, $O_2^{2-} \rightarrow$ Cu(II) [**4b** $\rightarrow \phi_S$], are both allowed under C_2 symmetry. In *Cancer* and *Busycon* hemocyanins, we assign **4b** $\rightarrow \phi_S$ at ~570 nm (2.18 eV) and **5a** $\rightarrow \phi_S$ at ~490 nm (2.53 eV). The higher energy transition is apparently weaker and not resolved in the room temperature absorption spectrum. The $O_2^{2-} \rightarrow$ Cu(II) electronic transitions reduce electron density localized in the antibonding orbitals of peroxide and lead to a strengthening of the O-O bond. For this reason, it is the O-O bond stretching vibration that is selectively enhanced in the Raman spectrum by laser excitation within the ~490-570-nm bands.

The proposed MO scheme also provides an explanation for the band at ~340 nm in hemocyanins. Oxygenation and the concomitant formation of Cu(II)-hemocyanin create a vacant ϕ_S orbital which, in turn, becomes a suitable terminal orbital for charge transfer from N(imidazole). The 340-nm transition thereby couples to the Cu-N(imidazole) vibrational mode observed in the Raman spectrum with blue-light excitation.

Copper-copper separations for the structure shown in Figure 4A range from 3.5 Å ($\alpha = 90°$, $\beta = 100°$) to 5 Å ($\alpha = 115°$, $\beta = 145°$) assuming Cu-O = 2.0 Å and O-O = 1.5 Å. The angles, $\alpha = 113°$ and $\beta = 146°$, are observed[52] in $[(NH_3)_5Co^{III}(O_2)Co^{III}(NH_3)_5]^{4+}$. If the Cu-Cu distance calculated from the EPR spectra of NO-hemocyanin,[33] ~6 Å, is similar to that of deoxyhemocyanin, the 3.5-5 Å separation calculated above implies a substantial movement of the copper ions upon oxygenation. Such a conformational change is consistent with hemocyanin oxygenation kinetics.[57]

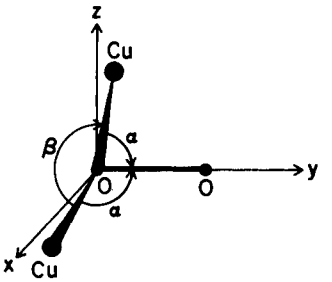

Figure 6. Geometry (IIb) for nonplanar, μ-monooxygen bridged Cu-O_2-Cu complex, C_s symmetry. α and β are the Cu-O-O and dihedral angles, respectively. This is an alternate structure to that illustrated in Figure 4A giving the analogous MO scheme (Figure 5) and spectral assignments (see text).

For a μ-monooxygen bridged structure with C_s symmetry, IIb (Figure 6), the MO scheme and assignments are entirely analogous to that presented above, replacing the a and b species designations of the C_2 point group with a′ and a″, respectively, for the C_s structure. However, the Cu-Cu separation would be somewhat smaller for this arrangement. A coplanar monooxygen bridged structure (IIa) where the copper d orbitals interact with only one π_g component is presumably less stable. The π-bridged geometry (Id) would also have a similar molecular orbital pattern, but this structure would be rather sterically strained and, thus, unfavorable.

For terminal oxygen binding (III), a molecular orbital diagram is less easily estimated than for either monooxygen or dioxygen bridging (I and II), since the ϕ_S, ϕ_A splitting would then be determined by some additional bridging group(s) in the protein. In this case, the oxidation to Cu(II) and the π_g splitting consistent with the assignment of the $O_2^{2-} \rightarrow$ Cu(II) charge transfer bands would be determined by the particular copper-oxygen geometry and bond strength. For π-bonded complexes

the O-O stretching frequencies lie 100-150 cm^{-1} higher[58] than that observed for oxyhemocyanin, making structure IIIb less likely. Although structure IIIa is certainly plausible on the basis of current information on the chemical and physical properties of hemocyanin, a recent x-ray crystallographic study on the structure of the iron-binding site in hemerythrin[59] appears to rule out terminal oxygen binding in that respiratory protein. In metaquohemerythrin, the Fe_2-complex can be viewed as two octahedra which appear to share a common face. Protein ligands appear to occupy all six terminal positions and two of the three bridging-coordination positions. On this basis, a structure involving bridged oxygen (as peroxide[26]) is most attractive.

Acknowledgments. We gratefully acknowledge the National Institutes of Health (GM 18865) and the Medical Research Foundation of Oregon for financial assistance of this research. We thank Professor Roald Hoffmann for making his manuscript available to us prior to its publication and Professor Kensal van Holde and Dr. David Ellerton for their unpublished

CD results on *C. magister* hemocyanin. The valuable assistance of Dr. Jeffrey Freedman during many phases of this work is deeply appreciated.

References and Notes

(1) Oregon Graduate Center
(2) Portland State University
(3) F. Ghiretti, Ed., "Physiology and Biochemistry of Hemocyanins", Academic Press, London, 1968.
(4) K. E. van Holde and E. F. J. van Bruggen in "Subunits in Biological Systems", Part A, S. N. Timasheff and G. D. Fasman, Ed., Marcel Dekker, New York, N.Y., 1971, pp 1–53.
(5) R. Lontie and L. Vanquickenborne in "Metal Ions in Biological Systems", Vol. 3, H. Sigel, Ed., Marcel Dekker, New York, N.Y., 1974, pp 183–200.
(6) K. E. van Holde, *Biochemistry*, **6**, 93 (1967).
(7) E. Frieden, S. Osaki, and H. Kobayashi, *J. Gen. Physiol.*, **49**, 213 (1965).
(8) T. H. Moss, D. C. Gould, A. Ehrenberg, J. S. Loehr, and H. S. Mason, *Biochemistry*, **12**, 2444 (1973).
(9) T. G. Spiro in "Chemical and Biochemical Applications of Lasers", Vol. 1, C. B. Moore, Ed., Academic Press, New York, N.Y., 1974, pp 29–70.
(10) J. S. Loehr, T. B. Freedman, and T. M. Loehr, *Biochem. Biophys. Res. Commun.*, **56**, 510 (1974).
(11) K. W. Nickerson and K. E. van Holde, *Comp. Biochem. Physiol. B*, **39**, 855 (1971).
(12) C. H. Ke and J. Schubert, *Radiat. Res.*, **49**, 507 (1972).
(13) C. Bonaventura, B. Sullivan, J. Bonaventura, and S. Bourne, *Biochemistry*, **13**, 4784 (1974).
(14) L. C. G. Thomson, M. Hines, and H. S. Mason, *Arch. Biochem. Biophys.*, **83**, 88 (1959).
(15) E. Ochiai, *Inorg. Nucl. Chem. Lett.*, **9**, 987 (1973).
(16) W. J. Eilbeck, F. Holmes, and A. E. Underhill, *J. Chem. Soc. A*, 757 (1967).
(17) D. M. L. Goodgame, M. Goodgame, and G. W. Rayner-Canham, *J. Chem. Soc. A*, 1923 (1971).
(18) A. Levitzki, I. Pecht, and A. Berger, *J. Am. Chem. Soc.*, **94**, 6844 (1972).
(19) H. A. de Phillips, Jr., K. W. Nickerson, and K. E. van Holde, *J. Mol. Biol.*, **50**, 471 (1970).
(20) R. C. Lord and N-T. Yu, *J. Mol. Biol.*, **50**, 509 (1970).
(21) A. Ghiretti-Magaldi, C. Nuzzolo, and F. Ghiretti, *Biochemistry*, **5**, 1943 (1966).
(22) J. S. Loehr and H. S. Mason, unpublished results, 1972.
(23) J. C. Evans, *Chem. Commun.*, 682 (1969).
(24) T. B. Freedman, C. M. Yoshida, and T. M. Loehr, *J. Chem. Soc., Chem. Commun.*, 1016 (1974).
(25) B. Salvato, A. Ghiretti-Magaldi, and F. Ghiretti, *Biochemistry*, **13**, 4778 (1974).
(26) J. B. R. Dunn, D. F. Shriver, and I. M. Klotz, *Proc. Nat. Acad. Sci., U.S.A.*, **70**, 2582 (1973).
(27) A. Y. Hirakawa and M. Tsuboi, *Science*, **188**, 359 (1975).
(28) A. C. Albrecht and M. C. Hutley, *J. Chem. Phys.*, **55**, 4438 (1971).
(29) W. J. Eilbeck, F. Holmes, C. E. Taylor, and A. E. Underhill, *J. Chem. Soc. A*, 128 (1968).
(30) W. J. Eilbeck, F. Holmes, C. E. Taylor, and A. E. Underhill, *J. Chem. Soc. A*, 1189 (1968).
(31) G. F. Bryce and F. R. N. Gurd, *J. Biol. Chem.*, **241**, 122 (1966).
(32) H. C. Freeman in "Inorganic Biochemistry", Vol. 1, G. L. Eichhorn, Ed., Elsevier, Amsterdam, 1973, pp 121–166.
(33) A. J. M. Schoot-Uiterkamp, H. vander Deen, H. J. C. Berendsen, and J. F. Boas, *Biochim. Biophys. Acta*, **372**, 407 (1974).
(34) E. J. Wood and W. H. Bannister, *Biochim. Biophys. Acta*, **154**, 10 (1968).
(35) Y. Engelborghs and R. Lontie, *Eur. J. Biochem.*, **39**, 335 (1973).
(36) J. R. Ferraro, "Low Frequency Vibrations of Inorganic and Coordination Compounds", Plenum Press, New York, N.Y., 1971.
(37) A. W. Herlinger, S. L. Wenhold, and T. V. Long, II, *J. Am. Chem. Soc.*, **92**, 6474 (1970).
(38) O. Sliman, N. M. Young, and P. R. Carey, *J. Am. Chem. Soc.*, **96**, 5583 (1974).
(39) N. Shaklai and E. Daniel, *Biochemistry*, **9**, 564 (1970).
(40) W. H. Bannister, P. Camilleri, and E. N. Chantler, *Comp. Biochem. Physiol. B*, **45**, 325 (1973).
(41) H. S. Mason in "Oxygen in the Animal Organism", F. Dickens and E. Neil, Ed., MacMillan, New York, N.Y., 1964, p 118.
(42) R. Malkin and B. G. Malmstrom, *Adv. Enzymol.*, **33**, 177 (1970).
(43) R. L. Jolley, Jr., L. H. Evans, N. Makino, and H. S. Mason, *J. Biol. Chem.*, **249**, 335 (1974).
(44) L. Rimai, R. G. Kilponen, and D. Gill, *J. Am. Chem. Soc.*, **92**, 3824 (1970)
(45) R. Mendelsohn, *Nature (London)*, **243**, 22 (1973).
(46) J. L. Lippert, L. E. Gorczyca, and G. Meiklejohn, *Biochim. Biophys. Acta*, **382**, 51 (1975).
(47) J. B. R. Dunn, D. F. Shriver, and I. M. Klotz, *Biochemistry*, **14**, 2689 (1975).
(48) L. Waxman, *J. Biol. Chem.*, **250**, 3796 (1975).
(49) L. Y. Fager and J. O. Alben, *Biochemistry*, **11**, 4786 (1972).
(50) P. J. Hay, J. C. Thibeault, and R. Hoffmann, *J. Am. Chem. Soc.*, **97**, 4884 (1975).
(51) B. M. Gimarc, *J. Am. Chem. Soc.*, **92**, 266 (1970).
(52) W. P. Schaefer, *Inorg. Chem.*, **7**, 725 (1968).
(53) U. Kaldor and I. Shavitt, *J. Chem. Phys.*, **44**, 1823 (1966).
(54) M. Kotani, Y. Mizuno, K. Kayama, and E. Ishiguro, *J. Phys. Soc. Jpn.*, **12**, 707 (1957).
(55) F. A. Cotton, C. B. Harris, and J. J. Wise, *Inorg. Chem.*, **6**, 909 (1967).
(56) E. I. Solomon, D. M. Dooley, R.-H. Wang, H. B. Gray, M. Cerdonio, F. Mogno, and G. L. Romani, *J. Am. Chem. Soc.*, **98**, 1029 (1976).
(57) M. Brunori, *J. Mol. Biol.*, **46**, 213 (1969).
(58) J. S. Valentine, *Chem. Rev.*, **73**, 235 (1973).
(59) R. E. Stenkamp, L. C. Sieker, and L. H. Jensen, *Proc. Natl. Acad. Sci. U.S.A.*, **73**, 349 (1976).

The Chemical Evolution of a Nitrogenase Model. XI. Reduction of Molecular Nitrogen in Molybdocyanide Systems

G. N. Schrauzer,* P. R. Robinson, E. L. Moorehead, and T. M. Vickrey

Contribution from the Department of Chemistry, The University of California at San Diego, Revelle College, La Jolla, California 92093. *Received September 22, 1975*

Abstract: Using $^{30}N_2$-enriched nitrogen as the substrate, the reduction of molecular nitrogen to ammonia is demonstrated in systems containing the complex anion $[Mo(O)(H_2O)(CN)_4]^{2-}$ and substrate amounts of ATP and $NaBH_4$. As in the molybdothiol model systems of nitrogenase, diimide, N_2H_2, is shown to be the first product of nitrogen reduction. The diimide subsequently disproportionates and in part decomposes to hydrazine, N_2 and H_2. Hydrazine is in turn reduced to ammonia; independent experiments show that this reaction is also catalyzed by molybdocyanide species and stimulated by ATP. The addition of ferredoxin model compounds as electron transfer catalysts enhances nitrogen reduction; CO, C_2H_2, CN^-, and O_2 cause partial or complete inhibition. The reduction of molecular nitrogen also occurs in systems containing MoO_4^{2-} and CN^- in the molar ratios of 1:1 or 1:2, in the presence of $NaBH_4$ and ATP.

In part X of this series[1] we demonstrated that the well-defined[2] complex $K_2[Mo(O)(H_2O)(CN)_4]$ may serve as a model for a substrate-catalyst complex in the simulation of the reduction of CN^- by nitrogenase (N_2-ase).[3,4] The coordinated CN^- in this anionic Mo^{4+} complex is reduced to NH_3, CH_4, C_2H_4, C_2H_6, and traces of CH_3NH_2 by reducing agents such as $NaBH_4$ or reduced ferredoxin model compounds. During the reaction, reactive cyanide complexes of oxomolybdate with free coordination sites are formed which catalyze the reduction of other substrates of N_2-ase, including molecular nitrogen. In part VII of this series it was shown that the reduction of N_2 in molybdothiol model systems of N_2-ase pro-